

Analytical Analysis of Axisymmetric Deep Drawing Process.

Najmeddin Arab^{1*}, and Ernest Nazaryan²¹Department of Material Science, Branch of Saveh, Azad Islamic University, Saveh, Iran.²Department of Physics, Yerevan State University, Yerevan, Armenia.

Research Article

Received: 26/06/2013

Revised: 02/07/2013

Accepted: 05/07/2013

***For Correspondence**Department of Material Science,
Branch of Saveh, Azad Islamic
University, Saveh, Iran.Keywords: Flanging, Sheet Metal
Forming, Thin Plates Forming, Deep
Drawing**ABSTRACT**

Mathematical description of the processes of sheet metal forming is very complicated process because of varying loading history and complex stress state in each point of material. The parameters for description of metal behaviour by the mathematical models of sheet metal forming are normally taken from a simplest mechanical test such as, for example, uniaxial traction test. Lately some new tests were developed which are closed to reel forming processes. Deep-drawing of a cylindrical cup occupies a particular place between these tests since it allows study the material work hardening, conditions of friction, springback, wrinkling, plastic flow instability, fracture and some others effects at the same time. In this research, deformation process of a thin ring plate with circular hole has been analyzed. By taking into account the thickness variations, and work hardening, the forming of thin ring plate at plane stress condition has been considered. It is shown that the deformation procedure of each point in the blank can be analysis by non-linear vector function of plasticity.

INTRODUCTION

Mathematical description of the processes of sheet metal forming is very complicated because of varying loading history and complex stress state in each point of material. The parameters for behavior law introduced in the mathematical models of sheet metal forming are normally taken from a simplest mechanical test such as, for example, uniaxial traction test. Lately some new tests were developed which are closed to reel forming processes. Deep-drawing of a cylindrical cup occupies a particular place between these tests since it allows to study material hardening, conditions of friction, springback, wrinkling, plastic flow instability, fracture and some others effects at the same time^[1,2]. There are two stages of deep-drawing during the first one the blank holder descends on a circular blank with special diameter and thickness and press it with special force, the process of forming takes place at the second stage when the cylindrical punch descends on the blank and draw it in the hole of matrix (figure 1). One can control the metal flow in matrix by modifying the blank-holder force that changes the friction force. Usually the process keeps on up to the moment of full drawing of the cup. But this is not always possible because of the fracture of the cup generally in the zone of cylindrical wall. It is obvious that the force of material resistance to drawing depends on the diameter of the initial blank against the punch diameter (R / R_0) - for bigger value of this ratio the force of resistance is bigger. Therefore there is a limiting drawing ratio (LDR) for which full cup drawing is still possible. In one of the first analytical models^[1] of this process Hill predicted the upper and the lower drawing limits for isotropic non-hardening material ($e = 1.65$ and $e = 2.72$ respectively). Later models^[3,4,5,6,7] improved this approach by considering the current geometry of the process (figure 1) in order to determine the strain rate field and then the stress field and the forces. In each of these models some simplifications were applied, in particular, the hypothesis of cup thickness unchanged during all the process. The current geometry of process when the punch has penetrated in matrix at a distance dm is presented in figure 1. Flange has an exterior diameter (changing in the time) equal to $2R_{ext}$, and interior diameter (which is unchanged) equal to $2R_{int}$. The radius of matrix and punch rims are r_p and r_m respectively. Force F_p , with which the punch acts on the blank increase at the beginning of process because of material hardening in flange and it decreases at the end of process as a result of flange reduction (figure 2).

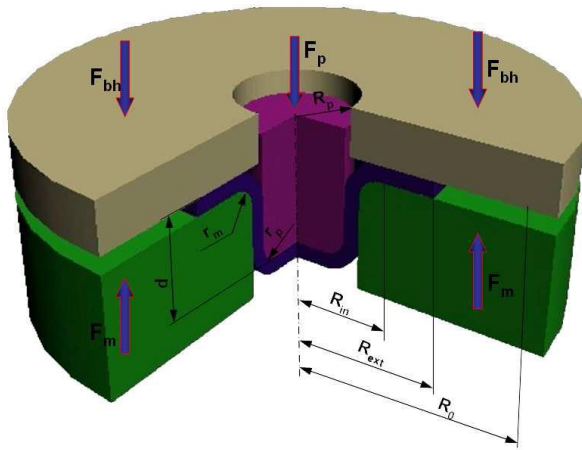


Figure 1: Schematic of deep drawing process.

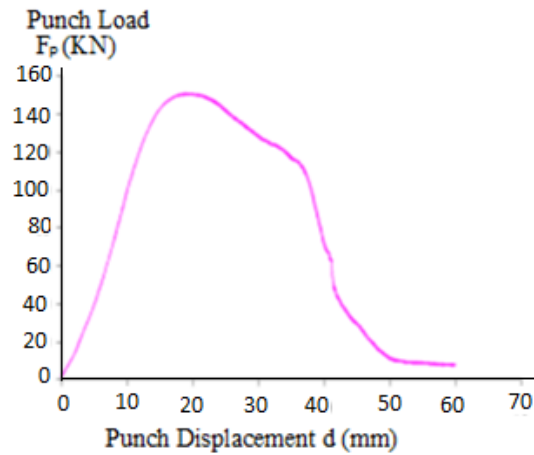


Figure 2: Punch load as a function of the punch displacement [8].

Analysis of flanging process

The present article is devoted to the theoretical analysis of flanging process of circular holes in thin plates taking into account the interconnected change of thickness and deformation hardening (when the known aspects of flanging process are omitted). Let's consider the forming process at flanging circular holes in thin plates, carried out by a punch with a flat end. In this research, it is shown that the initial equations characterize plastic plane stress state, taking place at flanging circular holes in thin plates,

- Equilibrium equation taking into account variability of thickness,
- coupling equation of pressure and deformation increments,
- Volume constancy condition ,
- Mises plasticity condition leads to a quite simple differential equation on deviatoric planes of plasticity:

$$d\sigma_p = \sigma_s d\epsilon_i \tag{Equation 1}$$

During derivation (1) radial σ_p and circumferential σ_θ pressure, which are expressed through the parameter of the deformed condition, are used in the given way:

$$\sigma_p = \frac{2}{\sqrt{3}} \sigma_s \cos(\varphi + \pi/6); \quad \sigma_\theta = -\frac{2}{\sqrt{3}} \sigma_s \sin \varphi \tag{Equation 2}$$

and the components of deformation increments are presented with the help of known equations

$$d\epsilon_p = d\epsilon_i \cos \varphi; \quad d\epsilon_\theta = d\epsilon_i \cos(\varphi + 2\pi/3); \quad d\epsilon_z = d\epsilon_i \cos(\varphi + 4\pi/3) \tag{Equation 3}$$

Components of deformation increments (3) unequivocally satisfy intensity of deformation increments, which, taking into account volume constancy condition, is defined by following expression

$$d\epsilon_i = \frac{2}{\sqrt{3}} \sqrt{d\epsilon_p^2 + d\epsilon_p d\epsilon_\theta + d\epsilon_\theta^2} \tag{Equation 4}$$

Isotropic deformation hardening is represented on the deviatoric plane of the plasticity cylinder in the form of circles with radiuses $\sigma_s/\sqrt{3}$ which increase in the radial direction by the size determined according to the value of accumulated deformation [9,10]

$$\sigma_s = A\epsilon_i^n \tag{Equation 5}$$

Where A, n are constants values of deformation hardening. The current value of accumulated deformation, taking into consideration the condition of volume constancy, is defined as:

$$\epsilon_i = \frac{2}{\sqrt{3}} \sqrt{\epsilon_\rho^2 + \epsilon_\rho \epsilon_\theta + \epsilon_\theta^2}$$

(Equation 6)

From comparison of equations (4) and (6) follows, that generally intensity of deformation increments $d\epsilon_i$ is not equal to the intensity increment $\bar{d}\epsilon_i$ defined by differentiation of equation (6). Therefore integration of the differential equation (1) taking into account (5) is possible only for the radial ways of deformations at which for the given material element the relation of the deformation increment components remains constant. Parameter ϕ change limits in the considered problem are determined, based on flanging process definition at which for all deformation site current sizes of circular deformations are positive, increasing from zero on the border of non-deformable part of the blank to the greatest value on the hole edge. From the analysis of equation (2) follows, that on border of not deformable part of blank radial stretching strain cannot exceed the value $2\sigma_s/\sqrt{3}$, corresponding to direction $\phi = 11\pi/6$ at which $\epsilon_\theta = 0$ and from the absence condition of radial stretching strain on the hole edge follows that the regional element is deformed under the conditions of circular stretching in the positive direction of axis ϵ_θ that corresponds to direction $\phi = 4\pi/3$. From abovementioned reasonings it follows that theoretically possible range of realisation of flanging process, at which current size of district deformation is $\epsilon_\theta \geq 0$ for all material elements, is located on deviatoric planes of plasticity cylinder within parameter change ϕ in the range $4\pi/3 \leq \phi \leq 11\pi/6$. Hence, all types of deformations in flanging process are completely characterised by the corners occupying a sector with central angle $\phi = \pi/2$ (figure 3).

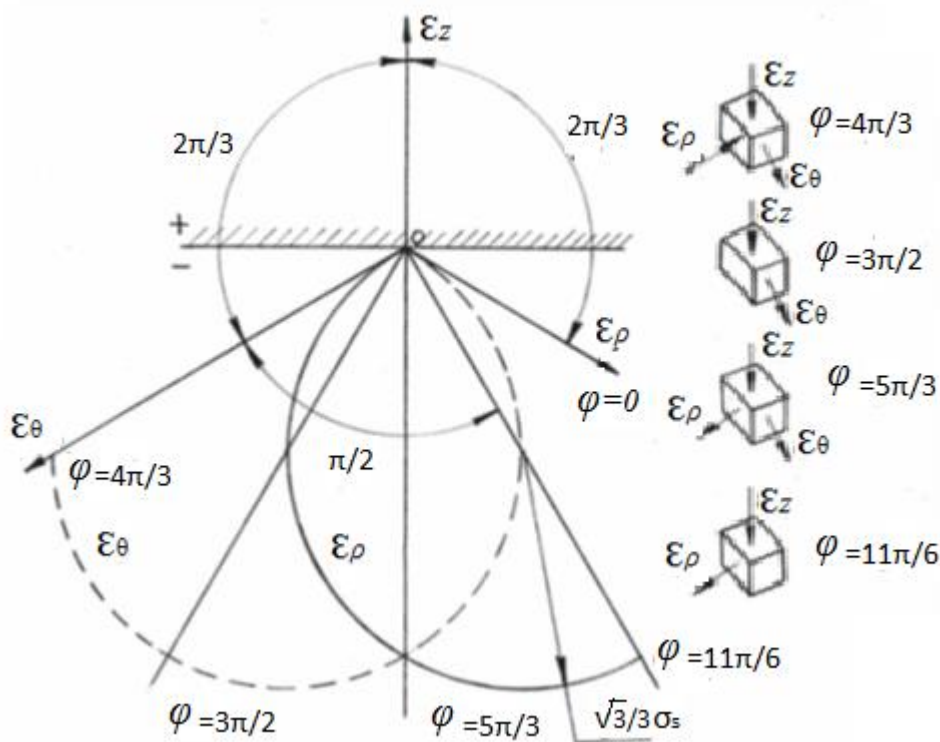


Figure 3: Modes of deformation and types of deformations at flanging.

If the deformation way coincides with axis ϵ_θ - stretching deformation in the circumferential direction, ϵ_ρ and ϵ_z compression deformations numerically equal $\epsilon_\theta / 2$. If the deformation way coincides with a negative direction of axis ϵ_z , then ϵ_z compression deformations by thickness, ϵ_ρ and ϵ_θ - the stretching deformations numerically equal $\epsilon_z / 2$. If the deformation way coincides with direction $\epsilon_\rho = 0$, ϵ_θ and ϵ_z are equal by size and are opposite on sign, pure shift or flat deformation in the plane (θ, Z) takes place. If the deformation way coincides with direction $\epsilon_\theta = 0$, ϵ_ρ and ϵ_z are equal by size and are opposite on sign, pure shift or flat deformation in the plane (ρ, Z) takes place. Thus, ways of deformation with corners $\phi = 3\pi/2$ and $11\pi/6$ correspond to pure shift, accordingly, in planes (θ, Z) and (ρ, Z) and with corners $\phi = 4\pi/3$ and $5\pi/3$ to pure stretching and compression, accordingly, in circumferential direction and in the direction of thickness. To determine the conformity between coordinates of considered elements and the parameter of the deformed condition we will integrate the equation (1) at earlier accepted assumption about radial character of current deformation accumulation that follows from the assumption about the parity constancy between pressures σ_ρ and σ_θ .

Equating result of integration to the value of radial pressure defined by equation (2) we get

$$\epsilon_i^{1+n} - \epsilon_{ip}^{1+n} = (1+n)\epsilon_i^n \frac{2}{\sqrt{3}} \cos(\phi + \pi/6)$$

(Equation 7)

At integration (1) the boundary condition is used, according to which for the boundary element

$\varepsilon_i = \varepsilon_k \rho$, $\varepsilon_\rho = 0$ (the hole edge is deformed in the circumferential direction in the conditions of linear stretching throughout the whole forming process). The known distribution of deformation intensity by the corner ϕ allows to determine interrelation between coordinate ρ of the considered element and parameter ϕ on deviatoric planes of the plasticity cylinder. For the initial stage of forming process

($\varepsilon_k \rho = 0$) having differentiated expression (7) and equated the received result to (3) ($d\varepsilon_i = d\varepsilon_i$, $d\varepsilon_\theta = d\rho/\rho$) [10], we receive:

$$d\varepsilon_\theta = \frac{d\rho}{\rho} = (1+n) \left(\sin \phi \cdot \cos \phi + \frac{\sqrt{3}}{2} \sin^2 \phi + \frac{\sqrt{3}}{6} \cos^2 \phi \right) d\phi \tag{Equation 8}$$

Expression (8) after integration will become:

$$\ln \rho = (1+n) \left(\frac{\sqrt{3}}{3} \phi - \frac{1}{4} \cos 2\phi - \frac{\sqrt{3}}{12} \sin 2\phi \right) + c \tag{Equation 9}$$

Where the constant of integration c is determined from boundary condition, according to which, at $\phi = 4\pi/3$, $\rho = r_0$ (r_0 – initial radius of the hole). Substituting the value of integration constant in (9), after simple transformations we will receive:

$$\frac{\rho}{r_0} = \exp(1+n) \left(\frac{\sqrt{3}}{3} (\phi - 4\pi/3) - \frac{1}{4} \cos 2\phi - \frac{\sqrt{3}}{12} \sin 2\phi \right) \tag{Equation 10}$$

From (10) it follows, that the deformation site has the greatest sizes at $\phi = 11\pi/12$ ($\varepsilon_\theta = 0$), $\rho = \rho_0$ ρ_0 – the radius of die hole) and is equal

$$\frac{\rho_0}{r_0} = \exp(1+n) \frac{\sqrt{3} \pi}{3 \cdot 2} \approx 2,475 \cdot (1+n) \tag{Equation 11}$$

At $n = 0$ the limiting value of relation ρ_0/r_0 coincides with the result of works [9–11] received when solving the problem taking into account change of thickness for ideally rigid plastic model of deformable material. Equation (10), which establishes unequivocal connection between initial co-ordinate of the considered element and parameter ϕ , allows to consider the flanging process dividing it into two stages. At the initial stage of deformation parallel to punch lowering, formation of plastic deformation site from external (on the die hole edge) to the internal border takes place.

Meanwhile the blank elements move in radial direction, and their thickness decreases. Hence, there is an element deformed in direction $\phi = 3\pi/2$, for which radial deformation is $\varepsilon_\rho = 0$ throughout the whole forming process. For definition of coordinate ρ of this element, substituting in (10) $\phi = 3\pi/2$, we will receive

$$\frac{\rho}{r_0} = \exp(1+n) \left(\frac{\sqrt{3} \pi}{3 \cdot 6} + \frac{1}{4} \right) \approx 1,737 \cdot (1+n) \tag{Equation 12}$$

Comparing the received result for the relative co-ordinate, which delimits the shortening area from lengthening in radial direction at $n = 0$, with result of work ($\rho/r_0 = 2$) which has been received without taking into consideration the thickness change and the influence of deformation hardening, we see, that in [12] it is a little overrated. Thus, all material elements with the relative coordinate less than the value defined (12), are shortened in radial direction, being exposed to radial compression, and elements with relative coordinate more than this value, are extended in radial direction, being exposed to a radial stretching. Hence, at calculation of parameters of flanging process it is necessary to proceed from the value of flanging coefficient. At small values of deformation flanging coefficient $\varepsilon_\rho \leq 0$ and the total flange height are less than the width flanging part of blank. At the big values of flanging

coefficient when in deformation site ϵ_p changes its sign, compression deformations in radial direction are somewhat compensated by stretching deformations, and it becomes possible to apply the calculation which follows from the equation of length of flange sweep on equatorial line and the width of flanged part of the blank. Knowing the character of deformation intensity distribution, it is possible to define deformation components:

$$\begin{aligned} \epsilon_\rho &= \frac{1+n}{2} \left(1 + \cos 2\varphi - \frac{\sqrt{3}}{3} \sin 2\varphi \right) \\ \epsilon_\theta &= -\frac{1+n}{2} \left(\cos 2\varphi + \frac{\sqrt{3}}{3} \sin 2\varphi \right) \\ \epsilon_z &= -\frac{1+n}{2} \left(1 - \frac{2\sqrt{3}}{3} \sin 2\varphi \right) \end{aligned}$$

(Equation 13)

RESULTS AND DISCUSSION

On figure 4 the graphs changes of deformation intensity and deformation components are presented at change of parameter ϕ in range $4\pi/3 \leq \phi \leq 11\pi/6$ for the initial stage of deformation ($\epsilon_{kp} = 0$) at $n = 0.2$. From equations (13) and figure 4 it follows that in the center of deformations some element with parameter of deformed condition $\phi = 19\pi/12$ at the initial moment of deformation receives the greatest circular deformation equal to $\sqrt{3}/3 (1+n)$. We find the relative coordinate of the material element which has received the greatest circular deformation from (10): $\rho/r_0 = 2.1(1+n)$.

At the second stage of deformation, parallel to the increase in current radius of hole edge, formation of flange vertical wall begins, and at the final moment of deformation all material elements receive the set deformation value in circular direction defined by the relation of values of the hole and the deforming tool. On fig. 5 ways and distributions of deformations are presented at different deformation values of the hole edge for deformation hardening parameter $n = 0.2$.

Taking into consideration that deformations cannot accept zero values on border of non-deformable blank part of preparation ($\phi = 11\pi/6$) step-wise, dashed lines on figure 5 mark the zone of smooth reduction of deformation intensity from current sizes to zero. At the second stage of deformation the forming process has strongly pronounced non-stationary character at which there is a continuous change of sizes of plastic deformation sites. The impossibility of definition of current values of deformation components from equation (7) analytically is connected with the impossibility of its representation in the form of explicit function from parameter ϕ and deformation value of the hole edge. Therefore definition of current values and character of change deformation components is carried

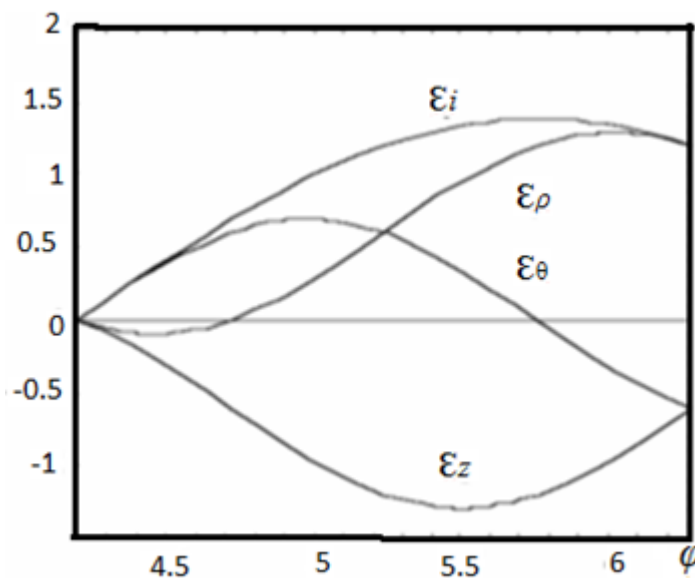


Figure 4: Distribution of deformation intensity at initial stage of deformation.

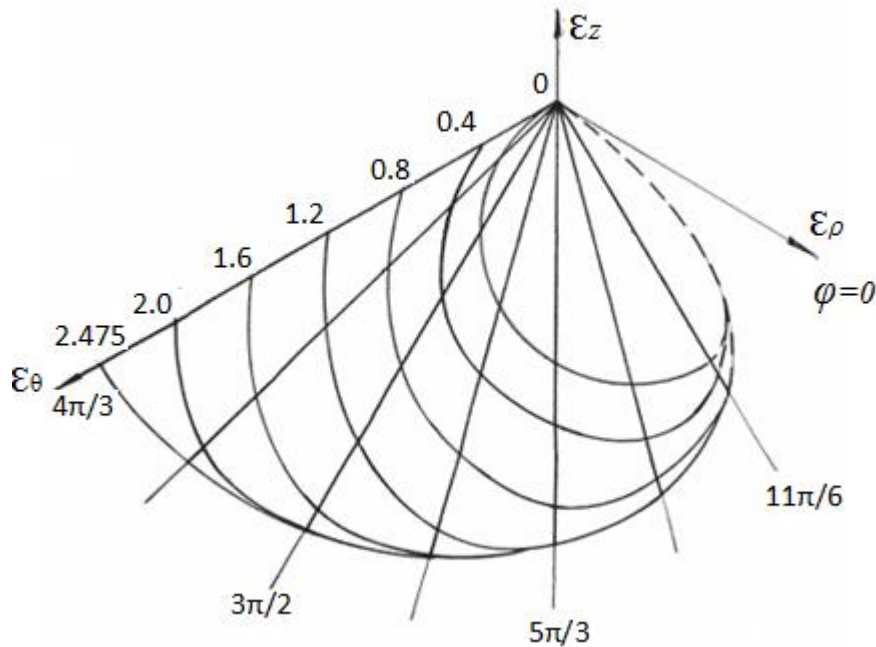


Figure 5:

Distribution of deformation at second Stage of deformation (curves of 1 and 2-7-Deformation distribution on initial and subsequent stages of deformation, directions $4\pi/3 \dots 11\pi/3$. Line no.8 is the greatest circular deformation) out by graphic projection of vector function $\bar{\epsilon}_i(\phi, \epsilon_{kp})$ on oblique-angled coordinate axes $\epsilon_\rho, \epsilon_\theta, \epsilon_z$ Graphs of change of current values of deformation components are presented on figure 5 at the variable deformation site for $n=0.2$.

Presented figures show that for the whole deformation site deformations by thickness are negative, whereas deformations in circular direction are positive. Radial deformations in direction $\phi = 3\pi/2$ change sign and, as a result, during the forming process one part of deformation site undergoes radial compression, and the other undergoes biaxial stretching.

REFERENCES

1. Hill R. The mathematical theory of plasticity, 1950, Oxford University Press,
2. Whiteley, R.L.; The Importance of Directionality in Drawing Quality Sheet Steel, Trans. American Society of Mechanical Engineers, 1960, 52, 154.
3. Baque P, Felder E, Hyafil J. Mise en forme des métaux (calcul par la plasticité) Tome 1. Edition Dunod, 1973.
4. Leu DK, The limiting ratio for plastic instability of the cup-drawing process. J Mat Proc Technol. 1999;86:168-176.
5. Verma RK, Chandra S. An improved model for predicting limiting drawing ratio. J Mat Proc Technol. 2006; 172: 218-224.
6. Springub B, Behrens BA. Semi-analytical identification of the flow curve extrapolation in consideration of martensite evolution. Proceedings of the IDDRG 2006 Conference, 19/06/2006-21/06/2006, Porto, 75-82
7. Schedin E. PhD, Thesis, Royal Institute of Technology, Stockholm, Sweden, 1991
8. Nazarov RA, Ayadi Z, Nikulin SA. Analytical model for deep-drawing of a cylindrical cup, NAME 2007
9. Nazaryan EA, Konstantinov VF. Kinematics of Straining in Deformation Operations of Sheet Stamping, Moscow. Bull Mach-Building. 1999;2:35-41.
10. Nazaryan EA, Konstantinov VF. Character of accumulation of deformations at plastic zone thin-wall sheets. J Blanking Prod Mech Eng. 2003;2:20-22.
11. Nazaryan EA, Arakelyan MM, Arab N. Deep drawing of hardly deformed sheet metals", International conference, IDDRG, 2007, Sweden.
12. Nazaryan EA, Kovalev V. etc.; Technology and automation of sheet punching process. Publishing house MGTU of Bauman University, Moscow, 2003, 480.